symmetry

MDPI

Article

From Probabilistic to Quantile-Oriented Sensitivity Analysis: New Indices of Design Quantiles

Zdeněk Kala

Department of Structural Mechanics, Faculty of Civil Engineering, Brno University of Technology, 602 00 Brno, Czech Republic; kala.z@fce.vutbr.cz

Received: 28 September 2020; Accepted: 15 October 2020; Published: 19 October 2020

Abstract: In structural reliability analysis, sensitivity analysis (SA) can be used to measure how an input variable influences the failure probability P_f of a structure. Although the reliability is usually expressed via P_f, Eurocode building design standards assess the reliability using design quantiles of resistance and load. The presented case study showed that quantile-oriented SA can provide the same sensitivity ranking as P_f-oriented SA or local SA based on P_f derivatives. The first two SAs are global, so the input variables are ranked based on total sensitivity indices subordinated to contrasts. The presented studies were performed for P_f ranging from 9.35×10^{-8} to 1–1.51×10^{-8}. The use of quantile-oriented global SA can be significant in engineering tasks, especially for very small P_f. The proposed concept provided an opportunity to go much further. Left-right symmetry of contrast functions and sensitivity indices were observed. The article presents a new view of contrasts associated with quantiles as the distance between the average value of the population before and after the quantile. This distance has symmetric hyperbola asymptotes for small and large quantiles of any probability distribution. Following this idea, new quantile-oriented sensitivity indices based on measuring the distance between a quantile and the average value of the model output are formulated in this article.

Keywords: sensitivity analysis; reliability; failure probability; quantile; civil engineering; limit states; mathematical model; uncertainty

1. Introduction

The reliability of building structures is influenced by inherent uncertainties associated with the material properties, geometry, and structural load variables to which the reliability measure is sensitive [1]. A common measure of reliability is the failure probability P_f, which is estimated using stochastic models [2]. Failure occurs when the load action is greater than the resistance. In this respect, the key issue is the identification of the significance of input random variables with regard to P_f.

Reliability-oriented sensitivity analysis (ROSA) consists of computing the sensitivity ranking of input variables ranked according to the amount of influence each has on P_f. It is argued that sensitivity analysis (SA) should be used "in tandem" with uncertainty analysis and the latter should precede the former in practical applications [3]. This can encumber the entire computational process, especially in cases of very small P_f.

Alternatively, the assessment of reliability can be performed by comparing the design quantiles of load and resistance [4,5]. A structure is reliable if the design resistance is greater than the design load action. One might ask, if the reliability assessment based on P_f can be replaced by a reliability assessment based on design quantiles, can the SA of P_f be replaced by the SA of design quantiles? For this purpose, new types of sensitivity indices oriented to both design quantiles and P_f can be investigated in engineering applications.

In civil engineering, classical Sobol SA (SSA) [6,7] is applied in the research of structural responses [8–16] or responses in geotechnical applications [17,18]. SSA is attractive for a number of reasons, e.g., it measures sensitivity across the whole input space (i.e., it is a global method), and it is capable of dealing with non-linear responses, as well as measuring the effect of interactions in non-additive models. However, SSA is based on the decomposition of variance of the model output, without a direct reference (only with partial empathy) to reliability [19].

Sobol indices in the context of ROSA can be derived as in [20], by introducing the binary random variable 1 (failure) or 0 (success) as the quantity of interest [21], where the basis of this transformation is the importance measure between P_f and conditional P_f defined in [22]. Indices can be derived in different variants, depending on whether the square of the importance measure [20] or the absolute value of the importance measure [23,24] is considered, but only the variant [20] after Sobol is based on decomposition, with the sum of all indices equal to one.

Both classical Sobol indices [6,7] and Sobol indices in the context of ROSA [20] are a subset of sensitivity indices subordinated to contrasts [25] (in short, Fort contrast indices). The general idea of Fort contrast indices [25] is that the importance of an input variable may vary, depending on what the quantity of interest is. Fort contrast indices define different types of indices based on a common platform, thus providing new perspectives on solving reliability tasks of different types.

It can be shown that Sobol indices in the context of ROSA [20] are Fort contrast indices [25] associated with P_f (referred to as contrast P_f indices in this article). Furthermore, it can be shown that the classical Sobol indices [6,7] are Fort contrast indices [25] associated with variance. In general, the type of Fort contrast index [25] varies, according to the type of contrast used. Contrast functions permit the estimation of various parameters associated with a probability distribution. By changing the contrast, SA can change its key quantity of interest. The contrast may or may not be reliability-oriented.

Fort contrast indices can be considered as global since they are based on changes of the key quantity of interest (P_f, α-quantile, variance, etc.) with regard to the variability of the inputs over their entire distribution ranges and they provide the interaction effect between different input variables. On the other hand, contrast functions account for the variability of the inputs regionally, according to the type of key quantity of interest, e.g., changes around the mean value are important for variance, changes around the quantile are important for the quantile, etc.

Standard [4] establishes the basis that sets out the way in which Eurocodes can be used for structural design. Although the concept of the probability-based assessment of structural reliability has been known about for a long time [5], new types of quantile-oriented SA have not yet been examined, in the context of structural reliability, at an appropriate depth. It can be expected that many of the reliability principles applied in [4] can be applied symmetrically in ROSA using new types of sensitivity indices to find new relationships. The introduced ROSA may be connected to decision-oriented methods [26] in areas of civil engineering, where decision-making under uncertainty is presently uncommon.

2. Probability-Based Assessment of Structural Reliability

Let the reliability of building structures be a one-dimensional random variable Z:

$$Z = g(X) = g(X_1, X_2, \ldots, X_M), \tag{1}$$

where $X_1, X_2, \ldots, X_M$ are random variables employed for its computation. The classical theory of structural reliability [27] expresses Equation (1) as a limit state using two statistically independent random variables, the load effect (action F), and the load-carrying capacity of the structure (resistance R).

$$Z = R - F \geq 0 \tag{2}$$

The variable that unambiguously quantifies reliability or unreliability is the probability that inequality (2) will not be satisfied. If Z is normally distributed, reliability index β is given as

$$\beta = \frac{\mu_Z}{\sigma_Z}, \tag{3}$$

where μ_Z is the mean value of Z and σ_Z is its standard deviation. By modifying Equation (3), we can express $\mu_Z - \beta \cdot \sigma_Z = 0$. The failure probability P_f can then be expressed as

$$P_f = P(Z < 0) = P(Z < \mu_Z - \beta \cdot \sigma_Z) = \Phi_U(-\beta), \tag{4}$$

where $\Phi_U(\cdot)$ is the cumulative distribution function of the normalized Gaussian probability density function (pdf). Reliability is defined as $P_s = (1 - P_f)$. For other distributions of Z, β is merely a conventional measure of reliability. Equation (3) can be modified for normally distributed Z, F, and R as

$$\beta = \frac{\mu_Z}{\sigma_Z} = \frac{\mu_R - \mu_F}{\sqrt{\sigma_R^2 + \sigma_F^2}} = \frac{\mu_R - \mu_F}{\frac{\sigma_R^2}{\sqrt{\sigma_R^2+\sigma_F^2}} + \frac{\sigma_F^2}{\sqrt{\sigma_R^2+\sigma_F^2}}} = \frac{\mu_R - \mu_F}{\alpha_R \cdot \sigma_R + \alpha_F \cdot \sigma_F}, \tag{5}$$

where α_F and α_R are values of the first-order reliability method (FORM) sensitivity factors.

$$\alpha_R = \frac{\sigma_R}{\sqrt{\sigma_R^2 + \sigma_F^2}}, \; \alpha_F = \frac{\sigma_F}{\sqrt{\sigma_R^2 + \sigma_F^2}}, \text{with } |\alpha| \le 1 \tag{6}$$

It can be noted that Sobol's first-order indices are equal to the squares of α_F and α_R: $S_F = \alpha_F^2$ and $S_R = \alpha_R^2$, respectively [19]. By applying α_F and α_R according to Equation (6), Equation (5) can be written with formally separated random variables as

$$\mu_F + \alpha_F \cdot \beta \cdot \sigma_F = \mu_R - \alpha_R \cdot \beta \cdot \sigma_R. \tag{7}$$

Equation (7) is a function of the four statistical characteristics of μ_F, σ_F, μ_R, and σ_R, from which β, α_F, and α_R are computed. The left side in Equation (7) is the design load F_d (upper quantile) and the right side is the design resistance R_d (lower quantile).

Standard [4] verifies the reliability by comparing the obtained reliability index β with the target reliability index β_d, according to the equation $\beta \ge \beta_d$, which transforms Equation (7) into the design condition of reliability:

$$\mu_F + \alpha_F \cdot \beta_d \cdot \sigma_F \le \mu_R - \alpha_R \cdot \beta_d \cdot \sigma_R, \tag{8}$$

where α_F and α_R may be considered as 0.7 and 0.8, respectively [4].

3. Sensitivity Analysis

In structural reliability, the key quantities of interest are the failure probability P_f and the design quantiles F_d and R_d. In order to analyse the reliability, ROSA must be focused on the same key quantity of interest: P_f, F_d, and R_d. Local and global types of ROSA are applied in this article.

3.1. Local ROSA

The partial derivative $\delta P_f / \delta \mu_{xi}$ with respect to the mean value μ of the input variable X_i presents a classical measure of change in P_f (see, e.g., [28–32]). The derivative-based approach has the advantage of being very efficient in terms of the computation time. There are two main disadvantages of using the derivative as an indicator of sensitivity.

The first disadvantage is that the derivative measures only change at the point (local SA) where it is numerically realized. If the algorithms on the computer are of the "black-box" type, then only a numerical evaluation of the derivative is possible. The second disadvantage is that a large absolute

value of the derivative does not necessarily mean a large influence of the input on the output if the distribution range of the input variable is small compared to other variables.

A better proportional degree of sensitivity is obtained when the derivative is multiplied by the standard deviation σ_{Xi} of the input variable.

$$D_i = \frac{\partial P_f}{\partial \mu_{X_i}} \sigma_{X_i} \tag{9}$$

The advantage of using Equation (9) is the inclusion of σ_{Xi} and the possibility of introducing a correlation between the input random variables. A limitation of the derivative-based approach occurs when the analysed variable is of an unknown linearity.

Regarding quantiles, the use of partial derivatives as an indicator of sensitivity analogously to Equation (9) is not offered. For example, for the additive model $X_1 + X_2$, the derivative of the quantile with respect to the mean value is always equal to one. Conversely, in non-additive models, the derivative of the quantile with respect to the mean value may give very high or low values, and thus, the derivative of the quantile does not appear to be a useful measure of sensitivity.

3.2. Global ROSA

Global ROSA can be computed using Fort contrast indices [25], which implicitly depend on parameters associated with the probability distribution. In engineering applications, it is primarily the probability P_f [33,34], the design quantiles F_d and R_d [35], or the median [36].

Sensitivity indices subordinated to contrasts associated with probability (in short, contrast P_f indices) are based on quadratic-type contrast functions [25]. However, contrast P_f indices can be defined more easily based on the probability of failure and the conditional probabilities of failure [19]. A formula that does not require the evaluation of contrast functions can be used for practical computation. For practical use, the first-order probability contrast index C_i can be rewritten in the form of [19]

$$C_i = \frac{P_f\left(1 - P_f\right) - E\left(\left(P_f|X_i\right)\left(1 - P_f|X_i\right)\right)}{P_f\left(1 - P_f\right)}. \tag{10}$$

The sensitivity index C_i measures, on average, the effect of fixing X_i on P_f, where $P_f = P(Z < 0)$ is the failure probability and $P_f|X_i = P((Z|X_i) < 0)$ is the conditional failure probability. The mean value E[·] is taken over X_i. In Equation (10), the term $P_f(1 - P_f)$ is derived for probability estimator θ^* = Argmin $\psi(\theta) = P_f$ from the minimum of contrast $\min_\theta \psi(\theta)$:

$$\min_\theta \psi(\theta) = \min_\theta E(\psi(Z, \theta)) = \min_\theta E(1_{Z<0} - \theta)^2 = \mathrm{V}(1_{Z<0}) = P_f\left(1 - P_f\right), \tag{11}$$

where V $(1_{Z<0})$ is the variance in the case where there are only two outcomes of 0 and 1, with one having a probability of P_f. The largest variance occurs if $P_f = 0.5$, with each outcome given an equal chance. The contrast function $\psi(\theta) = E(1_{Z<0} - \theta)^2$ vs. θ is convex and symmetrical in the interval across the vertical axis θ^*. The plot of $P_f(1 - P_f)$ vs. P_f is a concave function with left-right symmetry. The contrast for conditional probability is expressed in a similar manner as $(P_f|X_i)(1 - P_f|X_i)$.

The second-order sensitivity index C_{ij} is computed similarly:

$$C_{ij} = \frac{P_f\left(1 - P_f\right) - E\left(\left(P_f\middle|X_i, X_j\right)\left(1 - P_f\middle|X_i, X_j\right)\right)}{P_f\left(1 - P_f\right)} - C_i - C_j, \tag{12}$$

where $P_f|X_i,X_j = P((Z|X_i,X_j) < 0)$ is the conditional failure probability for fixed X_i and X_j. E[·] is taken over X_i and X_j. The index C_{ij} measures the joint effect of X_i and X_j on P_f minus the first-order effects of the same factors. The third-order sensitivity index C_{ijk} is computed similarly:

$$C_{ijk} = \frac{P_f\left(1-P_f\right) - E\left(\left(P_f\middle|X_i,X_j,X_k\right)\left(1-P_f\middle|X_i,X_j,X_k\right)\right)}{P_f\left(1-P_f\right)} - C_i - C_j - C_k - C_{ij} - C_{ik} - C_{jk}, \quad (13)$$

where $P_f|X_i,X_j,X_k = P((Z|X_i,X_j,X_k) < 0)$ is the conditional failure probability for fixed triples X_i, X_j, and X_k. The other indices are computed analogously. All input random variables are considered statistically independent. The sum of all indices must be equal to one:

$$\sum_i C_i + \sum_i \sum_{j>i} C_{ij} + \sum_i \sum_{j>i} \sum_{k>j} C_{ijk} + \ldots + C_{123\ldots M} = 1. \quad (14)$$

Contrast P_f indices can also be derived by rewriting Sobol indices in the context of ROSA [21]. Estimating all sensitivity indices in Equation (14) can be highly computationally challenging and difficult to evaluate. For a large number of input variables, it may be better to analyse the effects of input variables using the total effect index (in short, the total index) C_{Ti}.

$$C_{Ti} = 1 - \frac{P_f\left(1-P_f\right) - E\left(\left(P_f|X_{\sim i}\right)\left(1-P_f|X_{\sim i}\right)\right)}{P_f\left(1-P_f\right)} \quad (15)$$

$P_f|X_{\sim i} = P((Z|X_{\sim i}) < 0)$ is the conditional failure probability evaluated for a input random variable X_i and fixed variables $(X_1, X_2, \ldots, X_{i-1}, X_{i+1}, \ldots, X_M)$. The total index C_{Ti} measures the contribution of input variable X_i, including all of the effects caused by its interactions, of any order, with any other input variable. The total index C_{Ti} can also be computed if all sensitivity indices in Equation (14) are computed. For example, C_{T1} for $M = 3$ can be written as $C_{T1} = C_1 + C_{12} + C_{13} + C_{123}$.

The structural reliability can also be assessed using design quantiles (see, e.g., [37]). Sensitivity indices subordinated to contrasts associated with the α-quantile [25] (in short, contrast Q indices) are based on contrast functions of the linear type. The contrast function ψ associated with the α-quantile can be written with parameter θ as [25]

$$\psi(\theta) = E(\psi(Y,\theta)) = E((Y-\theta)(\alpha - 1_{Y<\theta})), \quad (16)$$

where Y is scalar (here, F or R). Equation (16) reaches the minimum if the argument θ is the α-quantile estimator θ^* (here, F_d or R_d). The plot of contrast function $\psi(\theta)$ vs. θ is convex and, with some exceptions, asymmetric.

Equation (16) is not quadratic like the contrast associated with P_f, because the distance $(Y - \theta)$ is considered linear. The first-order contrast Q index is defined, on the basis of Equation (16), as

$$Q_i = \frac{\min_\theta \psi(\theta) - E\left(\min_\theta E(\psi(Y,\theta)|X_i)\right)}{\min_\theta \psi(\theta)}, \quad (17)$$

where the first term in the numerator (and denominator) is the contrast computed for the estimator of α-quantile $\theta^* = \text{Argmin } \psi(\theta)$. The second term in the numerator is computed analogously, but with the provision that X_i is fixed. E[·] is taken over X_i.

The second-order α-quantile contrast index Q_{ij} is computed analogously, but with the fixing of pairs X_i and X_j:

$$Q_{ij} = \frac{\min\limits_{\theta}\psi(\theta) - E\left(\min\limits_{\theta}E\left(\psi(Y,\theta)\middle|X_i,X_j\right)\right)}{\min\limits_{\theta}\psi(\theta)} - Q_i - Q_j. \tag{18}$$

The third-order sensitivity index Q_{ijk} is computed similarly:

$$Q_{ijk} = \frac{\min\limits_{\theta}\psi(\theta) - E\left(\min\limits_{\theta}E\left(\psi(Y,\theta)\middle|X_i,X_j,X_k\right)\right)}{\min\limits_{\theta}\psi(\theta)} - Q_i - Q_j - Q_k - Q_{ij} - Q_{ik} - Q_{jk}. \tag{19}$$

All input random variables are considered statistically independent. The sum of all indices must be equal to one:

$$\sum_i Q_i + \sum_i \sum_{j>i} Q_{ij} + \sum_i \sum_{j>i} \sum_{k>j} Q_{ijk} + \ldots + Q_{123\ldots M} = 1. \tag{20}$$

The total index Q_{Ti} can be written analogously to Equation (15) as:

$$Q_{Ti} = 1 - \frac{\min\limits_{\theta}\psi(\theta) - E\left(\min\limits_{\theta}E(\psi(Y,\theta)|X_{\sim i})\right)}{\min\limits_{\theta}\psi(\theta)}, \tag{21}$$

where the second term in the numerator contains the conditional contrast evaluated for input random variable X_i and fixed variables (X_1, X_2, …, X_{i-1}, X_{i+1}, …, X_M). Equation (21) is analogous to Equation (15), but for the quantile.

3.3. Specific Properties of Contrasts Associated with Quantiles

Can contrast indices Q be estimated more easily, without having to evaluate the contrast function from Equation (16)? Let us study Equation (16) using a simple case study, where Y has a Gaussian pdf:

$$\phi(y,\ \mu,\ \sigma) = \frac{1}{\sigma\sqrt{2\pi}} e^{-\frac{(y-\mu)^2}{2\sigma}}. \tag{22}$$

Figure 1 depicts an example of the evaluation of the contrast function for the 0.4-quantile of the normalized Gaussian pdf—$Y \sim N(0, 1)$—where the 0.4-quantile is $\theta^* \approx -0.253$. The estimation of contrast function $\psi(\theta^*)$ is based on the dichotomy of the pdf into two parts, separated by the α-quantile.

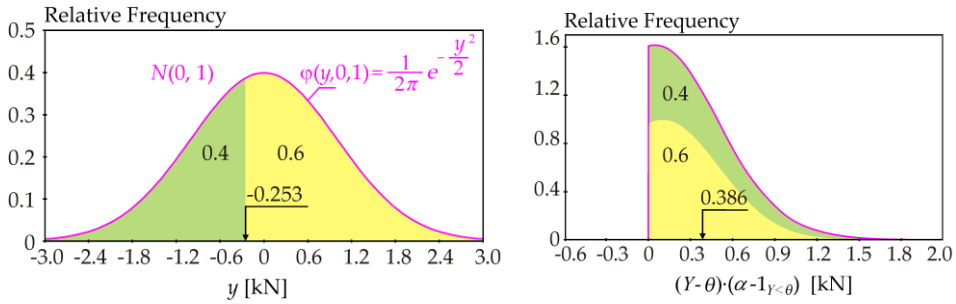

Figure 1. Example of the evaluation of Equation (16) for the 0.4-quantile of the Gaussian pdf.

The value of the contrast function in Equation (16) is $\psi(-0.253) = E((Y - (-0.253))(0.4-1_{Y<-0.253}))$ = 0.386, where the weight 0.6 favors the minority population over the 0.4-quantile and the weight 0.4 puts the majority population after the 0.4-quantile at a disadvantage. In this specific example, it can be observed that the function $\psi(\theta^*)$ vs. θ^* has an $N(0, 1)$ course and therefore, $\psi(-0.253) = \phi(-0.253,$

0, 1) = 0.386. In the case of the general Gaussian pdf $Y \sim N(\mu, \sigma^2)$, function $\psi(\theta^*)$ can be written in a specific form:

$$\psi(\theta^*) = \sigma^2 \cdot \phi(\theta^*, \mu, \sigma) = \frac{\sigma}{\sqrt{2\pi}} e^{-\frac{(\theta^*-\mu)^2}{2\sigma}}. \quad (23)$$

Equation (23) can only be used for estimates of contrast Q indices if Y has a Gaussian pdf; otherwise, Equation (23) has the form of an approximate relation. Another form of the sensitivity indices in Equation (20) derived from Equation (23) would be very practical; however, the conditional Gaussian pdf of Y, Gaussian pdf of $Y|X_i$, etc., makes the use of Equation (23) problematic in black box tasks, where skewness and kurtosis can have non-Gaussian values.

Due to the left-right symmetry of the Gaussian pdf in Figure 1, the same contrast function value can be obtained for the 0.6-quantile (see Figure 2).

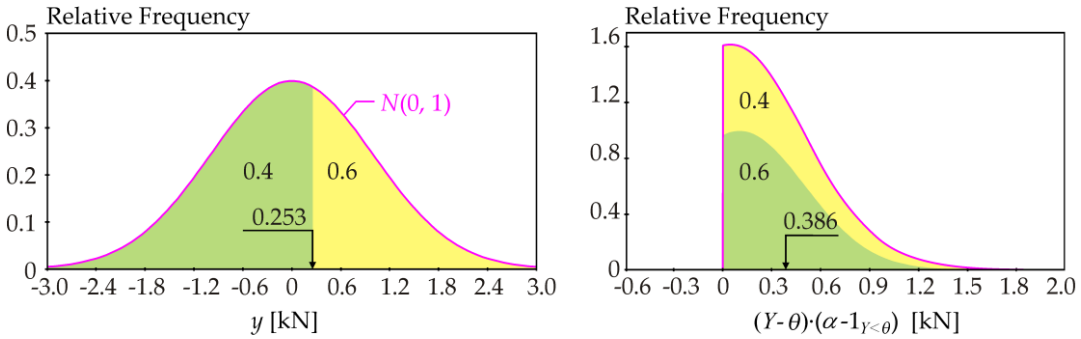

Figure 2. Example of the evaluation of Equation (16) for the 0.6-quantile of the Gaussian pdf.

The following approach is more powerful. The value of contrast function $\psi(\theta^*)$ can be expressed using the centers of gravity of the green and yellow areas (see Figure 3).

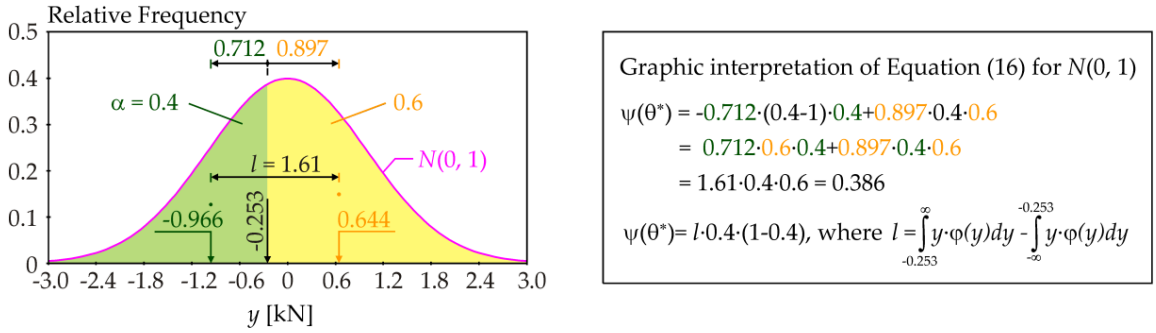

Figure 3. Graphical representation of the contrast in Equation (16) for the 0.4-quantile of $N(0, 1)$.

In the specific case of $Y \sim N(0, 1)$, the dependence between l and θ^* is a hyperbola $l^2 - (\theta^*)^2 \approx 1.6^2$ with asymptotes $l = \pm\theta^*$ (see Figure 4). In a more general case of $Y \sim N(\mu, \sigma^2)$, the dependence between l and θ^* is a hyperbola $l^2 - (\theta^* - \mu)^2 \approx \sigma^2 \cdot 1.6^2$ with asymptotes $l = \pm(\theta^* - \mu)$. The intersection of two asymptotes is at the center of symmetry of the hyperbola, which is the mean value $\mu = E(Y)$. The skewness and kurtosis (departure from the Gaussian pdf) lead to asymmetric and symmetric deviations from this hyperbola, but asymptotes of such a curve remain $l = \pm(\theta^* - \mu)$. Figure 4 illustrates an example with the so-called Hermite pdf with a mean value of 0, standard deviation of 1, skewness of 0.9, and kurtosis of 2.9. Although deviations from the hyperbola are significant around the mean value, the dependence l vs. θ^* approaches the asymptotes $l = \pm(\theta^* - \mu)$ in the regions of design quantiles (see Figure 4b). The observation can be generalized to any pdf or histogram of Y.

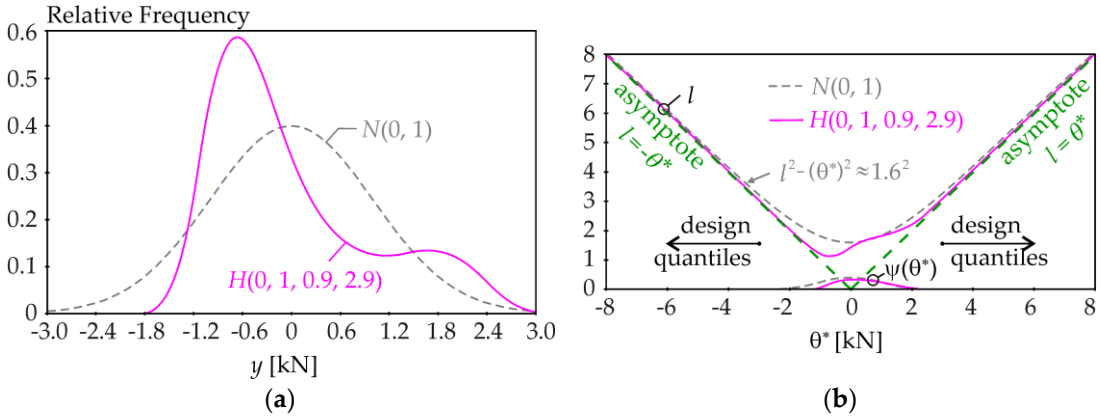

Figure 4. Plot of parameter l and function $\psi(\theta^*)$ vs. the α-quantile θ^*: (**a**) The Gaussian and non-Gaussian pdf; (**b**) The same asymptotes of hyperbolic and non-hyperbolic function.

For any pdf of $f(y)$ of Y, an alternative form of the contrast function to Equation (16) can be derived in a new form:

$$\psi(\theta^*) = l \cdot \alpha \cdot (1 - \alpha), \tag{24}$$

where l is the distance of the centers of gravity of the two areas before and after the α-quantile (see the example in Figure 3). Sensitivity indices reflect change around the α-quantile estimator θ^* using l while α is constant. Equation (24) is general for any pdf and offers new possibilities for evaluating contrast via l.

$$l = \int_{\theta^*}^{\infty} y \cdot f(y)dy - \int_{-\infty}^{\theta^*} y \cdot f(y)dy \tag{25}$$

In general, SSA is relevant to the mean value of Y, while the SA of the quantile (QSA) is relevant to the α-quantile of Y. However, in many cases, there is a strong similarity between the conclusions of QSA and SSA if all or at least the total sensitivity indices are examined. It can be shown in a simple example of $Y = X_1 + X_2$ that corr($Q(Y|X_i)$, $E(Y|X_i)$) ≈ 1, where $Q(Y|X_i)$ is the conditional α-quantile and $E(Y|X_i)$ is the conditional mean value. Changing X_i causes synchronous changes in the α-quantile $Q(Y|X_i)$ and mean value $E(Y|X_i)$.

Although contrasts are of a different type, similarities between the results of QSA and SSA have been observed in the task of SA of the resistance of a building load-bearing element [35]. Other numerical illustrations of contrast Q indices are presented in [38,39].

4. Case Study of the Ultimate Limit State

Probability-based reliability analysis considers a stochastic model of an ultimate limit state of a bar under tension (see Figure 5a). The structural member is safe when the sum of loads is less than the relevant resistance.

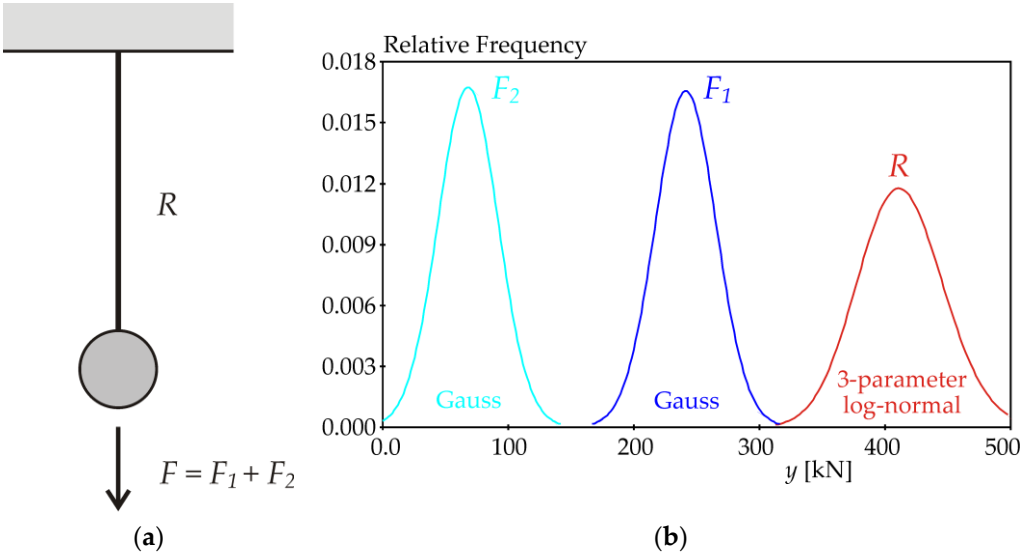

Figure 5. Static model: (**a**) Bar under tension and (**b**) probability density functions of R, F_1, and F_2 for $\mu_p = 0$.

The bar is loaded by two statistically independent forces F_1 and F_2, both of which have a Gaussian pdf (see Figure 5b and Table 1). Parameter μ_P changes the mean value of the axial load of the bar, while the standard deviation of F is constant. The resulting force $F = F_1 + F_2$ has a Gaussian pdf with a mean value of $\mu_F = \mu_{F_1} + \mu_{F_2} = 309.56$ kN + μ_P and standard deviation $\sigma_F = (\sigma_{F_1}^2 + \sigma_{F_2}^2)^{0.5} = 33.94$ kN.

Table 1. The input random variables on the load action side.

Characteristic	Index	Symbol	Mean Value μ (kN)	Standard Deviation σ
Load Action	1	F_1	241.4 + 0.5·μ_P	24.14 kN
Load Action	2	F_2	68.16 + 0.5·μ_P	23.86 kN

The stochastic computational model for the evaluation of the static resistance R is a function of three statistically independent random variables: The yield strength f_y; plate thickness t; and plate width b [40]:

$$R = f_y \cdot t \cdot b, \tag{26}$$

where t·b is the cross-sectional area. The resistance R is a function of material and geometric characteristics f_y, t, and b, whose random variabilities are considered according to the results of experimental research [41,42]. Random variables f_y, t, and b are statistically independent and are introduced with Gaussian pdfs (see Table 2).

Table 2. The input random variables on the resistance side.

Characteristic	Index	Symbol	Mean Value μ	Standard Deviation σ
Yield strength	3	f_y	412.68 MPa	27.941 MPa
Thickness	4	t	10 mm	0.46 mm
Width	5	b	100 mm	1 mm

The arithmetic mean μ_R, standard deviation σ_R, and standard skewness a_R of resistance R can be expressed using equations (see [40]), based on arithmetic means μ_{fy}, μ_t, and μ_b and standard deviations σ_{fy}, σ_t, and σ_b presented in Table 2.

The mean value of R can be written as

$$\mu_R = \mu_{fy} \cdot \mu_t \cdot \mu_b. \tag{27}$$

The standard deviation of R can be written as

$$\sigma_R = \sqrt{\mu_{fy}^2 \cdot \left(\mu_t^2 \cdot \sigma_b^2 + \sigma_t^2 \cdot \left(\mu_b^2 + \sigma_b^2\right)\right) + \mu_t^2 \cdot \sigma_{fy}^2 \cdot \left(\mu_b^2 + \sigma_b^2\right) + \sigma_{fy}^2 \cdot \sigma_t^2 \cdot \left(\mu_b^2 + \sigma_b^2\right)}. \tag{28}$$

The standard skewness of R can be written as

$$a_R = 6 \cdot \frac{\mu_R}{\sigma_R^3} \cdot \left(\mu_{fy}^2 \cdot \sigma_t^2 \cdot \sigma_b^2 + \sigma_{fy}^2 \cdot \mu_t^2 \cdot \sigma_b^2 + \sigma_{fy}^2 \cdot \sigma_t^2 \cdot \mu_b^2 + 4 \cdot \sigma_{fy}^2 \cdot \sigma_t^2 \cdot \sigma_b^2\right). \tag{29}$$

For example, for input random variables from Table 2, we can write μ_R = 412.68 kN, σ_R = 34.057 kN, and a_R = 0.111.

Goodness-of-fit and comparison tests [40] have shown that probabilities down to 1×10^{-19} are estimated relatively accurately using the approximation of probability density R by a three-parameter lognormal pdf with parameters μ_R, σ_R, and a_R. This approximation is also suitable when one variable in Equation (26) is fixed. Fixing two variables leads to R with a Gaussian pdf with parameters μ_R and σ_R.

In SA, the failure probability $P_f = P(Z < 0) = P(R < F)$ can be computed using distributions F (Gaussian) and R (three-parameter lognormal or Gaussian) as the integral:

$$P_f = \int_{-\infty}^{\infty} \Phi_R(y)\varphi_F(y)\mathrm{d}y, \tag{30}$$

where $\varphi_F(y)$ is the pdf of load action, $\Phi_R(y)$ is the distribution function of resistance, and y denotes a general point of the force (the observed variable) with the unit of Newton. The integration in Equation (30) is performed in the case study numerically using Simpson's rule, with more than ten thousand integration steps over the interval $[\mu_Z - 10\sigma_Z, \mu_Z + 10\sigma_Z]$.

5. Computation of Sensitivity Indices

The aim of SA in the presented case study is to assess the influence of input quantities F_1, F_2, f_y, t, and b on the failure probability P_f or design quantiles F_d and R_d.

The numerical parameter of the case study is μ_P, which changes with the step $\Delta\mu_P$ = 10 kN. Although μ_P is the computation parameter, sensitivity indices are preferably plotted, depending on P_f, because P_f has a clear relevance to reliability. The transformation of μ_P to P_f is expressed using Equation (30) (see Figure 6a).

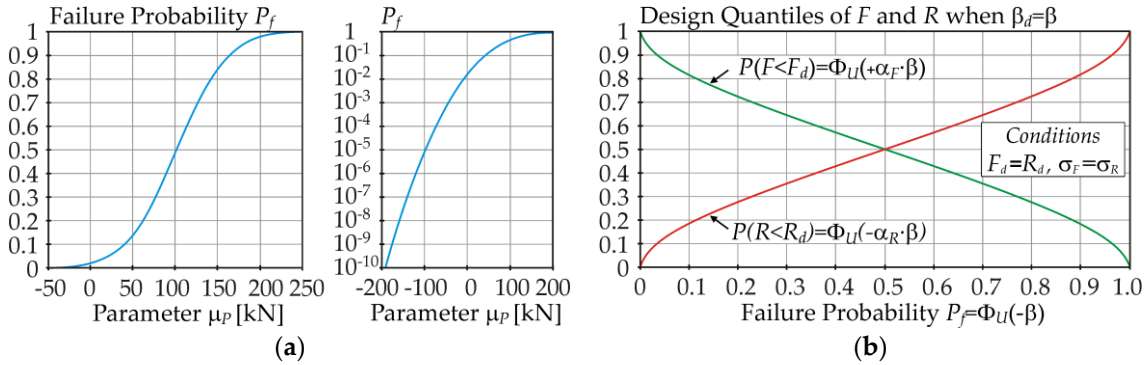

Figure 6. Probability of design α-quantiles vs. failure probability P_f: (**a**) μ_p vs. P_f; (**b**) P_f vs. α-quantiles.

In practice, the procedure is as follows: The value of μ_P is selected, the sensitivity indices and P_f are computed, and the indices vs. P_f are then plotted. If the design quantiles are the key quantities of interest, then the dependency between P_f and the probabilities of the design quantiles can be considered, according to Figure 6b.

In Figure 6b, the probability of design quantiles F_d and R_d is considered under the condition $F_d = R_d$ in Equation (7) and $\sigma_F = \sigma_R$. Perfect biaxial symmetry of the curves in Figure 6b is only observed for perfect $\sigma_F = \sigma_R$; otherwise, the curve of the variable with the smaller standard deviation has a steeper slope. In the case study, for $\beta = 3.8$ ($P_f = 7.2 \times 10^{-5}$), $P(F < F_d) = 0.9963$, and $P(R < R_d) = 0.0036$, where $F_d = R_d = 321.01$ kN ($\mu_F = 229.97$ kN, $\mu_R = 412.68$ kN, and $\sigma_F = 33.94$ kN $\approx \sigma_R = 34.057$ kN).

5.1. Local ROSA—Sensitivity Indices Based on Derivatives

Figure 7a shows the partial derivatives of P_f with respect to the mean values μ_{xi}. Although the partial derivative of P_f with respect to μ_t has the greatest value, t is not the most influential input variable in terms of the absolute change of P_f due to the uncertainty (variance) of the input variable t. A better measure of sensitivity is obtained by multiplying the partial derivatives by the standard deviations of the respective input variables (see Figure 7b). Ranking according to D_i gives the sensitivity ranking of input variables as f_y, F_1, F_2, t, and b.

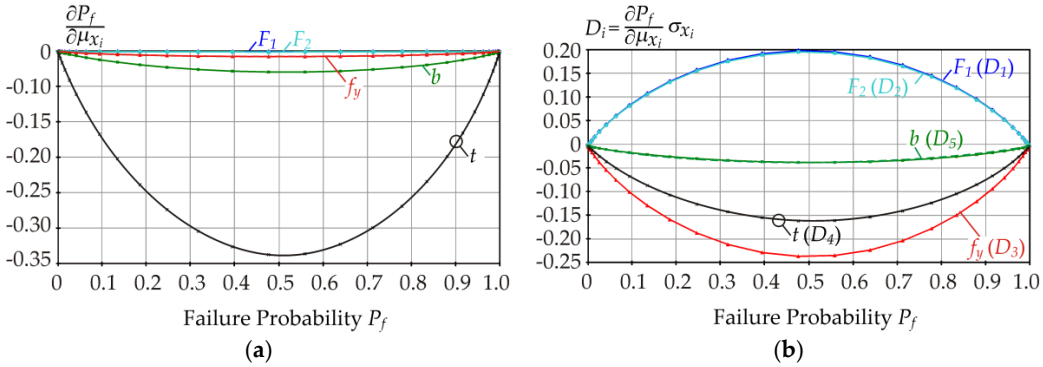

Figure 7. Derivative-based local SA of failure probability P_f: (**a**) Derivatives; (**b**) Sensitivity index D_i.

The plots in Figure 7 are approximately symmetrical about the vertical axis, but not perfectly symmetrical. The small amount of asymmetry is due to the small skewness of resistance R in Equation (1) (see Equation (29)). Perfect symmetry of the curves would occur if F and R had zero skewness (symmetric pdfs of both F and R).

A small amount of asymmetry is graphically visible upon mirroring the solid curves to the dashed curves (see Figure 8). The dashed curves are artificial, showing the left-right asymmetry of the solid curves.

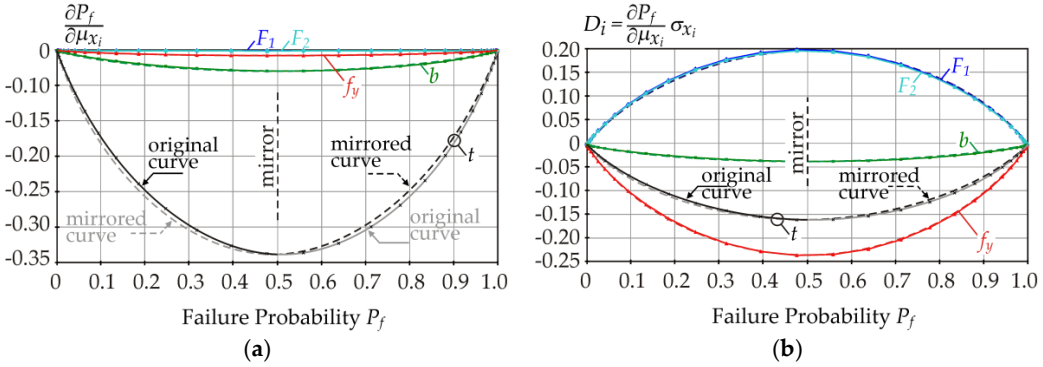

Figure 8. Derivative-based local SA of failure probability P_f: (**a**) Derivatives; (**b**) Sensitivity index D_i.

In Figure 8a, the dashed curves are lower than the solid curves on the left side of the graph. On the right side of the graph, the opposite is true. The same is observed in Figure 8b. A small amount of asymmetry occurs due to the small positive skewness of R. If R had a (theoretically) negative skewness, then the dashed curves would be higher than the solid curves on the left sides of each graph, and the opposite would be true on the right sides of the graphs.

5.2. Global ROSA—Contrast P_f Indices

For the case study, contrast P_f indices are depicted in Figures 9–13. All contrast P_f indices were computed numerically using Equation (30) for the interval $P_f \in [9.35 \times 10^{-8}, 1\text{–}1.51 \times 10^{-8}]$.

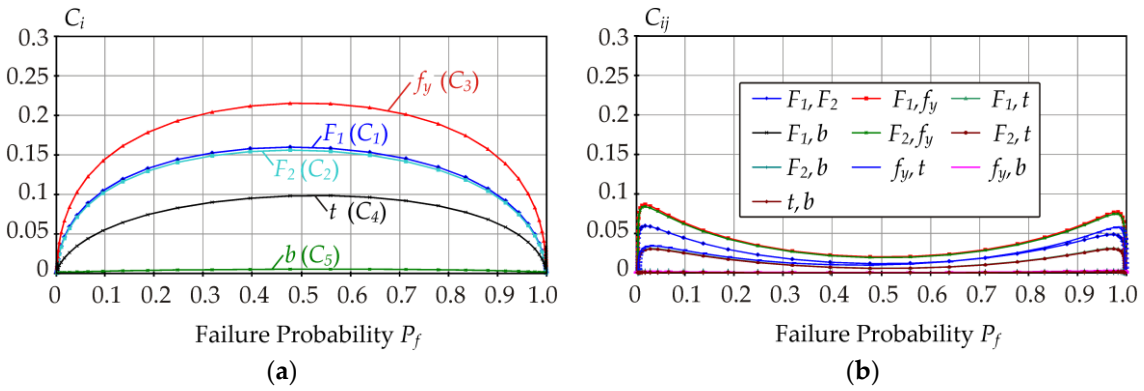

Figure 9. (**a**) First-order contrast P_f indices and (**b**) second-order contrast P_f indices.

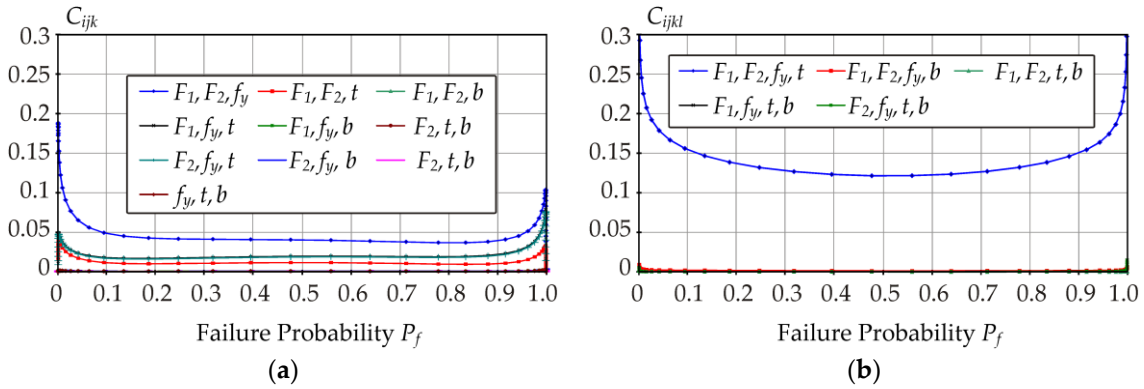

Figure 10. (**a**) Third-order contrast P_f indices and (**b**) fourth-order contrast P_f indices.

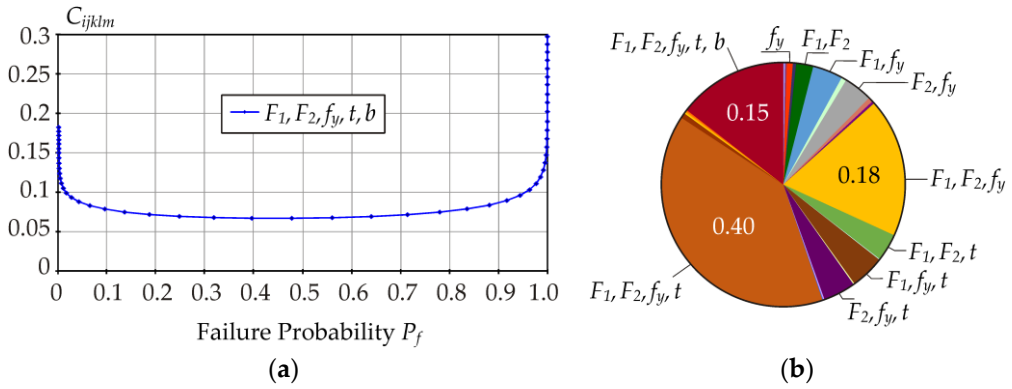

Figure 11. (**a**) Fifth-order contrast P_f indices and (**b**) all-order contrast P_f indices for $P_f = 7.2 \times 10^{-5}$.

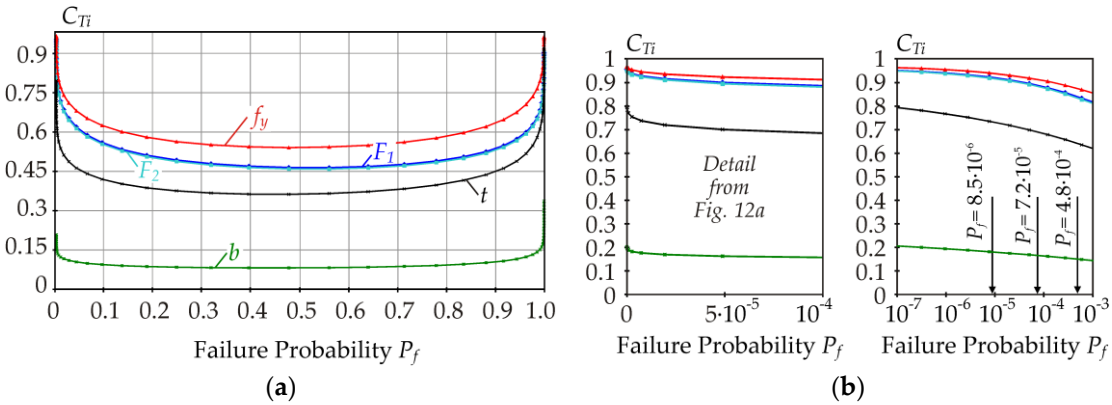

Figure 12. Total contrast P_f indices: (**a**) All P_f and (**b**) low P_f.

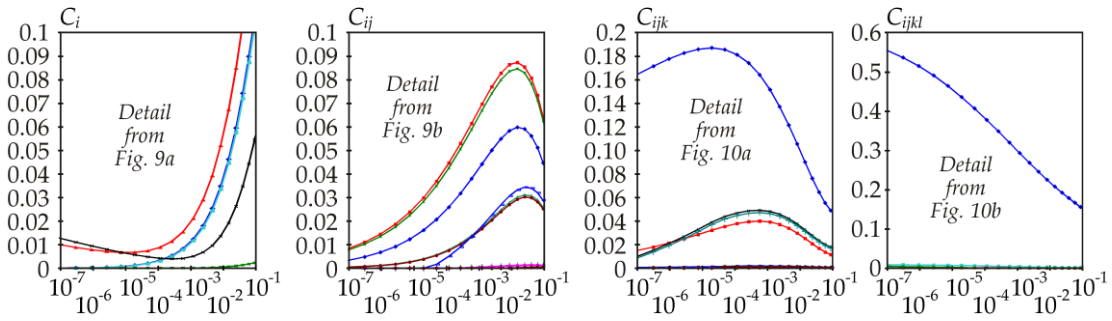

Figure 13. Details of contrast P_f indices for low P_f.

In the interval $P_f \in [0.1, 0.9]$, the plot of C_i is a concave function with approximately left-right symmetry. The sum of indices $C_1 + C_2$ is the same as what would have been obtained had we introduced only one random variable for F with a Gaussian pdf with a mean value of μ_F = 309.56 kN $+\mu_P$ and standard deviation of σ_F = 33.94 kN: $C_2 + C_1 = C_F$. The sum of indices $C_3 + C_4 + C_5$ is the same as what would have been obtained had we introduced only one random variable for R with a three-parameter lognormal pdf with parameters μ_R = 412.68 kN, σ_R = 34.057 kN, and a_R = 0.111: $C_3 + C_4 + C_5 = C_R$.

The slight asymmetry of the indices is of the same type as was described in the previous chapter for indices D_i. For example, for P_f = 0.3, indices C_1, C_2, and C_{12} (load action) have slightly smaller values and indices C_3, C_4, C_5, C_{34}, C_{35}, C_{45}, and C_{345} (resistance) have slightly higher values, compared to the perfect symmetry. For the other indices, there is a mix of both influences.

In the interval $P_f \in [0.1, 0.9]$, the first-, fourth-, and fifth-order indices generally have higher values than the second- and third-order indices.

In civil engineering, the target values of P_f for reliability classes RC1, RC2, and RC3 taken from [4] are 8.5×10^{-6}, 7.2×10^{-5}, and 4.8×10^{-4} (also see [19]). Figure 11b shows the contribution of all 31 indices for target value $P_f = 7.2 \times 10^{-5}$. First-order indices are represented minimally, where $\sum S_i = 0.017$. On the contrary, the representation of higher-order indices is significant, especially those related to f_y, F_1, and F_2 (see Figure 11b).

In Figure 11, f_y occurs in all significant parts of the graph, but the same is true for F_1 or F_2. Determining the order of importance of input variables using 31 indices can be difficult. The use of total indices C_{Ti} is more practical. Input variables are ranked based on C_{Ti} as f_y, F_1, F_2, t, and b (see Figure 12). This is the same ranking as was found using index D_i (Figure 7b).

Figure 12b shows the total sensitivity indices for small P_f, which are relevant for the design of building structures. Figure 13 shows the local extremes of some sensitivity indices in the interval of small P_f. Interestingly, the sensitivity indices of small P_f have plots that are not obvious (cannot be

extrapolated) from the plots in the interval $P_f \in [0.1, 0.9]$. Similar local extremes as in Figure 13 were not observed for D_i in Figure 7.

5.3. Global ROSA—Contrast Q Indices

In the case study, contrast Q indices were estimated using the Latin Hypercube Sampling (LHS) method [43,44], according to the procedure in [35]. Indices Q_i were estimated from Equation (17) using double-nested-loop computation. In the outer loop, E[·] was computed using one thousand runs of the LHS method. In the nested loop, conditional contrast values were computed using four million runs of the LHS method. The unconditional contrast value in the denominator was computed using four million runs of the LHS method. Higher-order indices were estimated similarly.

The target value $P_f = 7.2 \times 10^{-5}$ is considered according to [4]. In Equation (7), the design value of resistance R_d is considered as the 0.0036-quantile and the design load value F_d is considered as the 0.9963-quantile (see Figure 6). Sensitivity analysis is performed for R with a three-parameter lognormal pdf when no or one variable in Equation (26) is fixed; otherwise, a Gaussian pdf is used in the stochastic model.

It can be noted that standard design quantiles $F_d = R_d = 321.01$ kN computed using Equation (7) consider F and R with a Gaussian pdf. However, the design resistance value computed using a three-parameter lognormal pdf (stochastic model) is 325.00 kN. The small difference is because the skewness $a_R = 0.111$ was neglected in Equation (7).

The SA results of the 0.9963-quantile of F are depicted in Figure 14a. Input random variables for F are considered according to Table 1, where the value of μ_P for $P_f = 7.2 \times 10^{-5}$ is $\mu_P = -79.592$ kN. Input random variables for R are considered according to Table 2. The results of SA of the 0.0036-quantile of R are depicted in Figure 14b.

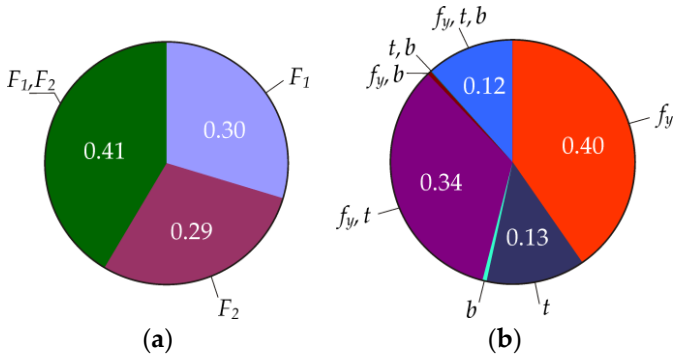

Figure 14. Contrast Q indices: (**a**) 0.9963-quantile of F and (**b**) 0.0036-quantile of R.

By computing total indices $Q_{T1} = 0.71$, $Q_{T2} = 0.70$ and $Q_{T3} = 0.86$, $Q_{T4} = 0.59$, and $Q_{T5} = 0.13$, the order of importance of input variables can be determined as F_1 and F_2 and f_y, t, and b. Variables F and R have the same weight in Equation (2) and therefore, the order of importance of all five input variables can be determined as f_y, F_1, F_2, t, and b, based on the estimates of all Q_{Ti}.

This is a typical example of how the ranking of input parameters based on total indices can give reliable results. The results are satisfactory, although ROSA is not evaluated directly using P_f; it is "only" based on the SA of design quantiles R_d and F_d.

In the presented study, the results for other values of the α-quantile are the same as in Figure 14. In practice, this means that the change in μ_P (generally a change in μ_F) is not reflected in the results of contrast Q indices.

6. New Sensitivity Indices of Small and Large Design Quantiles

6.1. The Asymptotic Form of Contrast Q Indices for Small and Large Quantiles

For small and large (design) quantiles, contrast Q indices can be rewritten using Equation (24) and the asymptotes of hyperbolic functions described in Chapter 3.3. The first-order contrast Q index can be rewritten as

$$Q_i = \frac{l \cdot \alpha \cdot (1-\alpha) - E((l|X_i) \cdot \alpha \cdot (1-\alpha))}{l \cdot \alpha \cdot (1-\alpha)} = \frac{l - E(l|X_i)}{l}. \tag{31}$$

By substituting the hyperbolic function $l^2 - (\theta^* - \mu)^2 = \sigma^2 \cdot l_0^2$ for l, we can obtain an approximate relation for Q_i:

$$Q_i \approx \frac{\sqrt{V(Y) \cdot l_0 + (Q(Y) - E(Y))^2} - E\left(\sqrt{V(Y|X_i) \cdot (l_0|X_i) + (Q(Y|X_i) - E(Y|X_i))^2}\right)}{\sqrt{V(Y) \cdot l_0 + (Q(Y) - E(Y))^2}}, \tag{32}$$

where $Q(Y) = \theta^*$, $E(Y) = \mu$, and $V(Y) = \sigma^2$. The non-dimensional parameter l_0 can be calculated from Equation (25) as $l_0 = l^2/\sigma^2$ at the point $\theta^* = \mu$. However, the precise value of l_0 is not important if $|Q(Y)\text{-}E(Y)|$ is large and l_0 does not affect the asymptotes. By substituting the hyperbolic functions with their asymptotes, Equation (31) can be simplified as

$$Q_i = \frac{l - E(l|X_i)}{l} \approx \frac{\left|Q(Y) - E(Y)\right| - E\left(\left|Q(Y|X_i) - E(Y|X_i)\right|\right)}{\left|Q(Y) - E(Y)\right|}. \tag{33}$$

Using asymptotes, the index is independent of variance and l_0. The second-order probability Q index can be rewritten analogously:

$$Q_{ij} \approx \frac{\left|Q(Y) - E(Y)\right| - E\left(\left|Q\left(Y\middle|X_i, X_j\right) - E\left(Y\middle|X_i, X_j\right)\right|\right)}{\left|Q(Y) - E(Y)\right|} - Q_i - Q_j. \tag{34}$$

The third-order probability Q index can be rewritten analogously:

$$Q_{ijk} \approx \frac{\left|Q(Y) - E(Y)\right| - E\left(\left|Q\left(Y\middle|X_i, X_j, X_k\right) - E\left(Y\middle|X_i, X_j, X_k\right)\right|\right)}{\left|Q(Y) - E(Y)\right|} - Q_i - Q_j - Q_k - Q_{ij} - Q_{ik} - Q_{jk} \tag{35}$$

Equations (33)–(35) represent an asymptotic form of contrast Q indices that can be used for SAs of low and high quantiles. Higher-order contrast Q indices can be rewritten analogously. The sum of all indices thus estimated is equal to one.

In civil engineering, the design quantile of resistance tends to be less than the 0.01-quantile and the design quantile of load action tends to be greater than the 0.99-quantile [4]. The asymptotic form of contrast Q indices reveals the degree of sensitivity as the distance between the quantile and the average value.

In the case study presented here, the use of Equation (33)–(35) leads to practically the same results as shown in Figure 14b, but only when low and high quantiles are analysed; otherwise, the formulas cannot be used. The computation of indices eliminates the repeated evaluation of contrast functions in the second loop.

6.2. New Quantile-Oriented Sensitivity Indices for Small and Large Quantiles: QE Indices

In Equation (33) to (35), replacing the absolute values with squares $(Q(Y) - E(Y))^2$, $(Q(Y|X_i) - E(Y|X_i))^2$, etc., leads to new sensitivity indices, which we denote as QE indices. The new first-order quantile-oriented index is defined as

$$K_i = \frac{(Q(Y) - E(Y))^2 - E\left((Q(Y|X_i) - E(Y|X_i))^2\right)}{(Q(Y) - E(Y))^2}. \tag{36}$$

The new second-order QE index is defined as

$$K_{ij} = \frac{(Q(Y) - E(Y))^2 - E\left(\left(Q\left(Y|X_i, X_j\right) - E\left(Y|X_i, X_j\right)\right)^2\right)}{(Q(Y) - E(Y))^2} - K_i - K_j. \tag{37}$$

The new third-order QE index is defined as

$$K_{ijk} = 1 - \frac{E\left(\left(Q\left(Y|X_i, X_j, X_k\right) - E\left(Y|X_i, X_j, X_k\right)\right)^2\right)}{(Q(Y) - E(Y))^2} - K_i - K_j - K_k - K_{ij} - K_{ik} - K_{jk}. \tag{38}$$

Sensitivity indices K_i, K_{ij}, and K_{ijk} were formulated via analogies to Equations (33)–(35) and were tested by numerical experiments using linear and non-linear Y functions and LHS simulations. Only low and high quantiles can be studied. The sum of the indices of all orders was equal to one in all cases. The total index K_{Ti} can be formulated analogously to Equation (21).

The new sensitivity indices can be explained using an analogy to Sobol sensitivity indices. The classical Sobol's first-order sensitivity index has the form

$$S_i = \frac{V(Y) - E(V(Y|X_i))}{V(Y)}. \tag{39}$$

Equation (36) can be interpreted using Equation (39). The key idea is to introduce l^2 as a variance. Equation (36) can be rewritten analogously to Equation (39) in the form

$$K_i = \frac{l^2 - E\left((l|X_i)^2\right)}{l^2}, \tag{40}$$

where l is the standard deviation of the "artificial" two-point probability mass function (pmf) having left-right symmetry around quantile $Q(Y)$ (see Figure 15). Half of the population is mirrored behind the quantile $Q(Y)$ and replaced by a dot on each side of $Q(Y)$. In SA, only low and high quantiles of Y can be analysed, indicating high l and low σ_Y in unconditional and conditional pdfs.

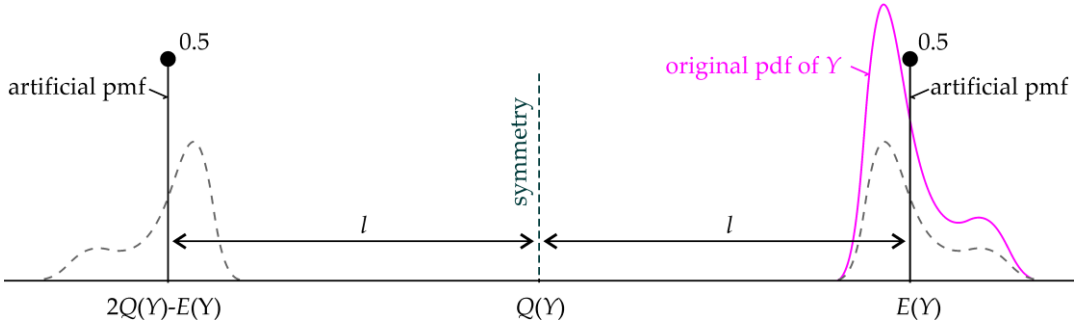

Figure 15. Introduction of l as the standard deviation of the two-point probability mass function.

Let $\mu_P = -79.592$ kN ($P_f = 7.2 \times 10^{-5}$). In the case study, QE indices were obtained on the load action side as $K_1 = 0.50$, $K_2 = 0.49$, and $K_{12} = 0.01$ and on the resistance side as $K_3 = 0.65$, $K_4 = 0.25$, $K_5 = 0.01$, $K_{34} = 0.08$, $K_{35} = 0.00$, $K_{35} = 0.00$, and $K_{345} = 0.01$ (see Figure 16). By computing the total indices $Q_{T1} = 0.51$, $Q_{T2} = 0.50$ and $Q_{T3} = 0.74$, $Q_{T4} = 0.34$, and $Q_{T5} = 0.02$, the order of importance of input variables can be determined as F_1 and F_2 and f_y, t, and b. The sensitivity ranking based on all five Q_{Ti} is f_y, F_1, F_2, t, and b.

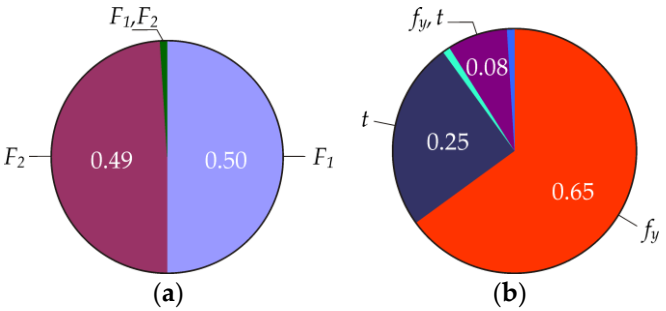

Figure 16. Contrast *QE* indices: (**a**) 0.9963-quantile of *F* ad (**b**) 0.0036-quantile of *R*.

7. Discussion

In the case study, input variables were listed in decreasing order of sensitivity as f_y, F_1, F_2, t, and b. Although the values of sensitivity indices of the different ROSA types vary, each ROSA gives the same sensitivity ranking:

- $Q_{T3} = 0.86 > Q_{T1} = 0.71 > Q_{T2} = 0.70 > Q_{T4} = 0.59 > Q_{T5} = 0.13$;
- $C_{T3} = 0.92 < C_{T1} = 0.892 < C_{T2} = 0.887 < C_{T4} = 0.69 < C_{T5} = 0.16$;
- $|D_3| = 1.64 \times 10^{-4} > |D_1| = 1.52 \times 10^{-4} > |D_2| = 1.50 \times 10^{-4} > |D_4| = 1.02 \times 10^{-4} > |D_5| = 0.21 \times 10^{-4}$;
- $K_{T3} = 0.74 > \mathrm{K_{T1}} = 0.51 > K_{T2} = 0.50 > K_{T4} = 0.34 > K_{T5} = 0.02$.

These results were obtained for $P_f = 7.2 \times 10^{-5}$ and the corresponding design quantiles (see previous sections). Contrast Q and P_f indices of higher-orders have a significant share in both types of ROSA; therefore, key information is provided by total indices. Regarding the sensitivity ranking, the total indices of design quantiles are a good proxy of the total indices of P_f. However, the result cannot be generalized beyond the Gaussian (or approximately Gaussian) design reliability conditions.

The proposed SA concept is applicable in tasks where the reliability can be assessed by comparing two α-quantiles of two statistically independent variables analogous to R and F (see Equation (2)). The pdfs of R and F should be close to Gaussian (see Equation (8)), with condition $\sigma_F \approx \sigma_R$. Then, ROSA can be effectively evaluated using the SA of design quantiles R_d and F_d, without having to analyse either P_f or the interactions between R and F. This is advantageous because estimates of contrast Q indices are usually numerically easier than estimates of contrast P_f indices, especially for small values of P_f.

For inequalities $\sigma_F \neq \sigma_R$, the total indices of design quantiles should be corrected using weights based on the sensitivity factors α_F and α_R from Equation (6). For example, if $\sigma_F \to 0$, then $\alpha_F \to 0$ and $\alpha_R \to 1$. When the influence of input variables on the load action side approaches zero, the reliability is only influenced by the variables on the resistance side. In the presented case study, the corrections of Q_{Ti} indices are as follows: $\alpha_F \cdot Q_{T1}$, $\alpha_F \cdot Q_{T2}$, $\alpha_R \cdot Q_{T3}$, $\alpha_R \cdot Q_{T4}$, and $\alpha_R \cdot Q_{T5}$. The correction of indices K_{Ti} can be performed similarly. If $\sigma_F = \sigma_R$, corrections are not necessary because $\alpha_F = \alpha_F = 0.7071$. Initial studies have shown the rationality of this approach; however, further analysis is necessary. Corrections of indices C_{Ti} are not performed. If $\sigma_F \to 0$, then C_{Ti} of the variables on the load action side approaches zero naturally. If an extreme value distribution is used, such as a Gumbel or Weibull pdf [45,46], then the proposed concept cannot be used.

Contrast Q indices are based on measuring the fluctuations around the quantile, which is the distance l between the average value of the population before and after the quantile (see Figure 3). For low and high quantiles, contrast Q indices can be rewritten using asymptotes $l = \pm\theta^*$ of hyperbolic functions (see Figure 4). Although contrast Q indices do not have an analogy to the variance decomposition offered by Sobol's indices through the Hoeffding theorem, studies of contrasts in applications [35,36] show some similarities between contrast Q indices and Sobol's indices. The new QE indices and Sobol's indices have formulas based on the squares of the distances from the average value and therefore, their comparison may be interesting in further work.

It can be noted that QE indices K_i, K_{ij}, and K_{ijk} give significant values of first-order indices K_i (compared to Q_i) and relatively small values of higher-order indices, which is also a property observed in Sobol's indices in the case study [35]. QE indices are based on quadratic measures of sensitivity like Sobol, but associated with quantiles. This domain deserves much more work in order to make QE indices a useful and practical tool.

All of the presented techniques are appropriate for SA of the stochastic model type considered in this article. For a general model, an important criterion is also the ease with which the SA can be performed. The most fundamental aspect of sensitivity techniques is local SA based on partial derivatives for computing the rate of change in P_f with respect to a given input parameter. Although the sensitivity ranking determined on the basis of D_i is the same as from C_{Ti}, Q_{Ti}, or K_{Ti}, this conclusion cannot be generalized, and D_i is not suitable for application in every task. The one-at-a-time techniques are only valid for small variabilities in parameter values or linear computation models; otherwise, the partials must be recalculated for each change in the base-case scenario. In contrast, contrast-based SA does not have these limitations because computational models can generally be non-linear and sensitivity indices take into account the variability of inputs throughout their distribution range and provide interaction effects between different input variables.

The results of ROSA can be compared with traditional SA techniques, such as the correlation between input X_i and output Z. Spearman's rank correlation coefficients are computed using one million LHS runs as corr(X_1, Z) = −0.49, corr(X_2, Z) = −0.48, corr(X_3, Z) = 0.56, corr(X_4, Z) = 0.38, and corr(X_5, Z) = 0.08. The second traditional SA technique is SSA. Sobol's first-order indices S_i are computed according to Equation (39), using double-nested-loop computation [35], whereas the inner loop has four million runs and the outer loop ten thousand runs. The model output is Z. The values of S_i are $S_1 = 0.25$, $S_2 = 0.24$, $S_3 = 0.34$, $S_4 = 0.16$, and $S_5 = 0.01$. Sobol's higher-order sensitivity indices are negligible. Both the correlation and SSA give the same sensitivity ranking as ROSA: f_y, F_1, F_2, t, and b. The case study shows that the normalization of the newly proposed indices K_{Ti} leads to the classical S_i, i.e., $K_{Ti}/2.11 \approx S_i$. Although correlations and Sobol's indices are commonly used in SA of the limit states of structures, neither is directly reliability-oriented [19]. Further analysis of the relationship between the new QE indices and traditional Sobol indices is needed because it can provide new insights into the use of SSA in reliability tasks.

The dominance of the yield strength is an important finding for static tensile tests of steel specimens in the laboratory. In structural systems, the slender members under compression may be influenced by other initial imperfections, such as bow and out-of-plumb imperfections [9,10]. In a general steel structure, these imperfections can change the order of importance of the input random variables.

Symmetry is an important part of sensitivity indices and contrast functions (see, e.g., Equation (11) or Equation (24)). Reliability $P_{\sim f} = (1 - P_f)$ or unreliability P_f leads to the same contrast P_f indices, because $P_f(1 - P_f) = P_{\sim f}(1 - P_{\sim f})$. In the case study, the plots of the sensitivity indices were slightly asymmetric due to the small values of skewness of R. The plots of sensitivity indices vs. P_f would be perfectly symmetric in the case of a perfectly symmetric pdf of R and F, with zero skewness.

In the presented study, conclusions were made using SA subordinated to a contrast [25] and SA based on partial derivatives of P_f and new types of QE indices. Other types of SA of P_f like [47] or SA of the quantile [48] have not been studied. Numerous other types of sensitivity measures exist, such as [49–59], and it cannot be expected that the conclusions would be confirmed using any sensitivity

index. The advantage of SA subordinated to a contrast is the use of a single platform (contrast) for the analysis of different parameters associated with a probability distribution.

8. Conclusions

This article has examined the relationships between the principles of semi-probabilistic reliability assessment of building structures according to the EN1990 standard and reliability-oriented sensitivity analysis (ROSA). The probability distributions of load and resistance close to Gaussian have been considered.

The article proposes new tools for performing ROSA. It has been shown that ROSA can be credibly evaluated using total indices of quantiles of resistance and load action, without the need to study the failure probability. ROSA of design quantiles gives the same sensitivity ranking as the two types of ROSA oriented to failure probability. Although this conclusion has been established based on one case study, the initial results suggest the possibility of using quantile-oriented ROSA in structural reliability studies. It should be interesting to develop a general approach for determining how to combine the various known indices, and in what order, in order to tackle a reliability task.

New quantile-oriented sensitivity indices denoted as QE indices have been formulated in the article. The first study showed that the distance between the quantile and the average value can be a very interesting measure of sensitivity, with the possibility of further development.

The apparent efforts to develop new types of sensitivity analyses show that the scientific community is still looking for the right combination of computational methods to solve specific problems. An important problem in structural reliability analysis is how to reduce the failure probability. Research focused on design quantities complements the development of failure probability estimation methods.

In engineering applications, the inclusion of quantile-oriented sensitivity analysis among the tools for assessing the effects of input variables on reliability makes it possible to effectively reduce the computational cost of sensitivity analysis of reliability with numerically demanding models. An example is the sensitivity analysis of design quantiles of numerous load cases, where the design quantile of the resistance of a structure only needs to be analysed once. It is worth noting that the specification of which parameters constantly appear close to the top of the list with the order of sensitivity is more important than the actual ranking. In practice, we can neglect the discrepancy between rankings for less important variables because these variables have a minimal or no effect on the reliability of structures.

Funding: The work has been supported and prepared within the project named "Influence of material properties of stainless steels on reliability of bridge structures" of The Czech Science Foundation (GACR, https://gacr.cz/), No. 20-00761S, Czechia.

Conflicts of Interest: The author declares no conflict of interest.

References

1. Ditlevsen, O.; Madsen, H. *Structural Reliability Methods*; John Wiley & Sons Inc.: New York, NY, USA, 1996.
2. Au, S.-K.; Wang, Y. *Engineering Risk Assessment with Subset Simulation*; Wiley: New York, NY, USA, 2014.
3. Antucheviciene, J.; Kala, Z.; Marzouk, M.; Vaidogas, E.R. Solving civil engineering problems by means of fuzzy and stochastic MCDM methods: Current state and future research. *Math. Probl. Eng.* **2015**, *2015*, 362579. [CrossRef]
4. European Committee for Standardization. *EN 1990:2002: Eurocode—Basis of Structural Design*; European Committee for Standardization: Brussels, Belgium, 2002.
5. Joint Committee on Structural Safety (JCSS). Probabilistic Model Code. Available online: https://www.jcss-lc.org/ (accessed on 15 May 2020).
6. Sobol, I.M. Sensitivity estimates for non-linear mathematical models. *Math. Model. Comput. Exp.* **1993**, *1*, 407–414.

7. Sobol, I.M. Global sensitivity indices for nonlinear mathematical models and their Monte Carlo estimates. *Math. Comput. Simul.* **2001**, *55*, 271–280. [CrossRef]
8. Kala, Z. Sensitivity assessment of steel members under compression. *Eng. Struct.* **2009**, *31*, 1344–1348. [CrossRef]
9. Kala, Z. Sensitivity analysis of steel plane frames with initial imperfections. *Eng. Struct.* **2011**, *33*, 2342–2349. [CrossRef]
10. Kala, Z. Global sensitivity analysis in stability problems of steel frame structures. *J. Civ. Eng. Manag.* **2016**, *22*, 417–424. [CrossRef]
11. Kala, Z.; Valeš, J. Global sensitivity analysis of lateral-torsional buckling resistance based on finite element simulations. *Eng. Struct.* **2017**, *134*, 37–47. [CrossRef]
12. Xiao, S.; Lu, Z.; Wang, P. Global sensitivity analysis based on distance correlation for structural systems with multivariate output. *Eng. Struct.* **2018**, *167*, 74–83. [CrossRef]
13. Zamanian, S.; Hur, J.; Shafieezadeh, A. Significant variables for leakage and collapse of buried concrete sewer pipes: A global sensitivity analysis via Bayesian additive regression trees and Sobol' indices. *Struct. Infrastruct. Eng.* **2020**, 1–13. [CrossRef]
14. Carneiro, G.D.; Antonio, C.C. Sobol' indices as dimension reduction technique in evolutionary-based reliability assessment. *Eng. Comput. Swans.* **2020**, *37*, 368–398. [CrossRef]
15. El Kahi, E.; Deck, O.; Khouri, M.; Mehdizadeh, R.; Rahme, P. Simplified probabilistic evaluation of the variability of soil-structure interaction parameters on the elastic transmission of ground movements. *Eng. Struct.* **2020**, *213*, 110554. [CrossRef]
16. Jafari, M.; Akbari, K. Global sensitivity analysis approaches applied to parameter selection for numerical model-updating of structures. *Eng. Comput.* **2019**, *36*, 1282–1304. [CrossRef]
17. Štefaňák, J.; Kala, Z.; Miča, L.; Norkus, A. Global sensitivity analysis for transformation of Hoek-Brown failure criterion for rock mass. *J. Civ. Eng. Manag.* **2018**, *24*, 390–398. [CrossRef]
18. Xu, Z.X.; Zhou, X.P.; Qian, Q.H. The uncertainty importance measure of slope stability based on the moment-independent method. *Stoch. Environ. Res. Risk Assess.* **2020**, *34*, 51–65. [CrossRef]
19. Kala, Z. Sensitivity Analysis in Probabilistic Structural Design: A Comparison of Selected Techniques. *Sustainability* **2020**, *12*, 4788. [CrossRef]
20. Wei, P.; Lu, Z.; Hao, W.; Feng, J.; Wang, B. Efficient sampling methods for global reliability sensitivity analysis. *Comput. Phys. Commun.* **2012**, *183*, 1728–1743. [CrossRef]
21. Li, L.; Lu, Z.; Feng, J.; Wang, B. Moment-independent importance measure of basic variable and its state dependent parameter solution. *Struct. Saf.* **2012**, *38*, 40–47. [CrossRef]
22. Cui, L.; Lu, Z.; Fhao, X. Moment-independent importance measure of basic random variable and its probability density evolution solution. *Sci. China Technol. Sci.* **2010**, *53*, 1138–1145. [CrossRef]
23. Xiao, S.; Lu, Z. Structural reliability sensitivity analysis based on classification of model output. *Aerosp. Sci. Technol.* **2017**, *71*, 52–61. [CrossRef]
24. Ling, C.; Lu, Z.; Cheng, K.; Sun, B. An efficient method for estimating global reliability sensitivity indices. *Probabilistic Eng. Mech.* **2019**, *56*, 35–49. [CrossRef]
25. Fort, J.C.; Klein, T.; Rachdi, N. New sensitivity analysis subordinated to a contrast. *Commun. Stat. Theory Methods* **2016**, *45*, 4349–4364. [CrossRef]
26. Zavadskas, E.K.; Antucheviciene, J.; Vilutiene, T.; Adeli, H. Sustainable decision-making in civil engineering, construction and building technology. *Sustainability* **2018**, *10*, 14. [CrossRef]
27. Freudenthal, A.M. Safety and the probability of structural failure. *Trans. ASCE* **1956**, *121*, 1337–1375.
28. Melchers, R.E.; Ahammed, M. A fast-approximate method for parameter sensitivity estimation in Monte Carlo structural reliability. *Comput. Struct.* **2004**, *82*, 55–61. [CrossRef]
29. Ahammed, M.; Melchers, R.E. Gradient and parameter sensitivity estimation for systems evaluated using Monte Carlo analysis. *Reliab. Eng. Syst. Safe.* **2006**, *91*, 594–601. [CrossRef]
30. Millwater, H. Universal properties of kernel functions for probabilistic sensitivity analysis. *Probabilistic Eng. Mech.* **2009**, *24*, 89–99. [CrossRef]
31. Wang, P.; Lu, Z.; Tang, Z. A derivative based sensitivity measure of failure probability in the presence of epistemic and aleatory uncertainties. *Comput. Math. Appl.* **2013**, *65*, 89–101. [CrossRef]
32. Zhang, X.; Liu, J.; Yan, Y.; Pandey, M. An effective approach for reliability-based sensitivity analysis with the principle of Maximum entropy and fractional moments. *Entropy* **2019**, *21*, 649. [CrossRef]

33. Kala, Z. Global sensitivity analysis of reliability of structural bridge system. *Eng. Struct.* **2019**, *194*, 36–45. [CrossRef]
34. Kala, Z. Estimating probability of fatigue failure of steel structures. *Acta Comment. Univ. Tartu. Math.* **2019**, *23*, 245–254. [CrossRef]
35. Kala, Z. Quantile-oriented global sensitivity analysis of design resistance. *J. Civ. Eng. Manag.* **2019**, *25*, 297–305. [CrossRef]
36. Kala, Z. Benchmark of goal oriented sensitivity analysis methods using Ishigami function. *Int. J. Math. Comput. Methods* **2018**, *3*, 43–50.
37. Jönsson, J.; Müller, M.S.; Gamst, C.; Valeš, J.; Kala, Z. Investigation of European flexural and lateral torsional buckling interaction. *J. Constr. Steel Res.* **2019**, *156*, 105–121. [CrossRef]
38. Browne, T.; Fort, J.-C.; Iooss, B.; Le Gratiet, L. Estimate of quantile-oriented sensitivity indices. *HAL* **2017**, hal-01450891.
39. Maume-Deschamps, V.; Niang, I. Estimation of quantile oriented sensitivity indices. *Stat. Probab. Lett.* **2018**, *134*, 122–127. [CrossRef]
40. Kala, Z. Limit states of structures and global sensitivity analysis based on Cramér-von Mises distance. *Int. J. Mech.* **2020**, *14*, 107–118. [CrossRef]
41. Melcher, J.; Kala, Z.; Holický, M.; Fajkus, M.; Rozlívka, L. Design characteristics of structural steels based on statistical analysis of metallurgical products. *J. Constr. Steel Res.* **2004**, *60*, 795–808. [CrossRef]
42. Kala, Z.; Melcher, J.; Puklický, L. Material and geometrical characteristics of structural steels based on statistical analysis of metallurgical products. *J. Civ. Eng. Manag.* **2009**, *15*, 299–307. [CrossRef]
43. McKey, M.D.; Beckman, R.J.; Conover, W.J. Comparison of the three methods for selecting values of input variables in the analysis of output from a computer code. *Technometrics* **1979**, *21*, 239–245.
44. Iman, R.C.; Conover, W.J. Small sample sensitivity analysis techniques for computer models with an application to risk assessment. *Commun. Stat. Theory Methods* **1980**, *9*, 1749–1842. [CrossRef]
45. Nadarajah, S.; Pogány, T.K. On the characteristic functions for extreme value distributions. *Extremes* **2013**, *16*, 27–38. [CrossRef]
46. Keshtegar, B.; Gholampour, A.; Ozbakkaloglu, T.; Zhu, S.-P.; Trung, N.-T. Reliability analysis of FRP-confined concrete at ultimate using conjugate search direction method. *Polymers* **2020**, *12*, 707. [CrossRef] [PubMed]
47. Shi, Y.; Lu, Z.; Zhao, L. Global sensitivity analysis of the failure probability upper bound to random and fuzzy inputs. *Int. J. Fuzzy Syst.* **2019**, *21*, 454–467. [CrossRef]
48. Kucherenko, S.; Song, S.; Wang, L. Quantile based global sensitivity measures. *Reliab. Eng. Syst. Saf.* **2019**, *185*, 35–48253. [CrossRef]
49. Saltelli, A.; Ratto, M.; Andres, T.; Campolongo, F.; Cariboni, J.; Gatelli, D.; Saisana, M.; Tarantola, S. *Global Sensitivity Analysis: The Primer*; John Wiley & Sons: West Sussex, UK, 2008.
50. Rykov, V.; Kozyrev, D. On the reliability function of a double redundant system with general repair time distribution. *Appl. Stoch. Models Bus. Ind.* **2019**, *35*, 191–197. [CrossRef]
51. Shahnewaz, M.; Islam, M.S.; Tannert, T.; Alam, M.S. Flange-notched wood I-joists reinforced with OSB collars: Experimental investigation and sensitivity analysis. *Structures* **2019**, *19*, 490–498. [CrossRef]
52. Douglas-Smith, D.; Iwanaga, T.; Croke, B.F.W.; Jakeman, A.J. Certain trends in uncertainty and sensitivity analysis: An overview of software tools and techniques. *Environ. Model. Softw.* **2020**, *124*, 104588. [CrossRef]
53. Kaklauskas, A.; Zavadskas, E.K.; Radzeviciene, A.; Ubarte, I.; Podviezko, A.; Podvezko, V.; Kuzminske, A.; Banaitis, A.; Binkyte, A.; Bucinskas, V. Quality of city life multiple criteria analysis. *Cities* **2018**, *72 Pt A*, 82–93. [CrossRef]
54. Lellep, J.; Puman, E. Plastic response of conical shells with stiffeners to blast loading. *Acta Comment. Univ. Tartu. Math.* **2020**, *24*, 5–18. [CrossRef]
55. Medina, Y.; Muñoz, E. A Simple time-varying sensitivity analysis (TVSA) for assessment of temporal variability of hydrological processes. *Water* **2020**, *12*, 2463. [CrossRef]
56. Mohebby, F. Function estimation in inverse heat transfer problems based on parameter estimation approach. *Energies* **2020**, *13*, 4410. [CrossRef]
57. Strauss, A.; Moser, T.; Honeger, C.; Spyridis, P.; Frangopol, D.M. Likelihood of impact events in transport networks considering road conditions, traffic and routing elements properties. *J. Civ. Eng. Manag.* **2020**, *26*, 95–112. [CrossRef]

58. Su, L.; Wang, T.; Li, H.; Cao, Y.; Wang, L. Multi-criteria decision making for identification of unbalanced bidding. *J. Civ. Eng. Manag.* **2020**, *26*, 43–52. [CrossRef]
59. Szymczak, C.; Kujawa, M. Sensitivity analysis of free torsional vibration frequencies of thin-walled laminated beams under axial load. *Contin. Mech. Thermodyn.* **2020**, *32*, 1347–1356. [CrossRef]